Published in final edited form as:
Plast Reconstr Surg. 2011 July ; 128(1): 114–121. doi:10.1097/PRS.0b013e31821741d4.

Dose-Response Effect of Human Equivalent Radiation in the Murine Mandible. Part I. A Histomorphometric Assessment

Catherine N. Tchanque-Fossuo, MD, MS,
University of Michigan Medical School, Ann Arbor, MI

Laura A. Monson, MD,
University of Michigan Medical School, Ann Arbor, MI

Aaron S. Farberg, BS,
University of Michigan Medical School, Ann Arbor, MI

Alexis Donneys, MD, MS,
University of Michigan Medical School, Ann Arbor, MI

Aria J. Zehtabzadeh,
University of Michigan Medical School, Ann Arbor, MI

Elizabeth R. Razdolsky, and
University of Michigan Medical School, Ann Arbor, MI

Steven R. Buchman, MD
University of Michigan Medical School, Ann Arbor, MI

Abstract

Background—Our lab previously demonstrated that radiation significantly alters new bone formation in the murine mandible impeding the use of distraction osteogenesis (DO) as a viable reconstructive option after radiatiotherapy in Head and Neck Cancer (HNC). We hypothesize that the deleterious effects of radiation on regenerate formation results from a dose response (DR) depletion of essential osteogenic cells. Our specific aim is to use quantitative histomorphometry (QHM) to objectively measure the human equivalent DR effects of radiation on the integrity of the mandible's cellular and tissue composition.

Methods—20 Sprague-Dawley rats were randomIzed into three radiation dosage groups: low (5.91Gy), middle (7Gy) and high (8.89Gy) delivered in 5 daily fractions. These dosages approximated 75%, 100%, and 150% respectively of the bioequivalent dose the mandible experiences in the clinical regimen of HNC patients. Hemimandibles were harvested 56 days post-radiation, and stained with Gomori Trichrome. QHM was performed using Bioquant software and analysis with a one-way ANOVA Kruskal-Wallis test.

Steven R. Buchman, M.D., Craniofacial Anomalies Program, Pediatric Plastic Surgery, 1500 E. Medical Center Drive, F7894 Mott Children's Hospital, Ann Arbor, Michigan 48109-5219, sbuchman@med.umich.edu.

Financial Disclosure and Products page
None of the authors has a financial interest in any of the products, devices, or drugs mentioned in this manuscript.

From the University of Michigan, Division of Plastic Surgery, Craniofacial Research Laboratory. Presented at the 55th Annual Meeting of the Plastic Surgery Research Council, in San Francisco, California, May 2010.

Results—Our data revealed a statistically significant diminution in the mean number of osteocytes . We also demonstrated a corresponding significant increase in the mean values of empty lacunae. Both of these QHM changes demonstrated a DR relationship.

Conclusion—Our study supports our hypothesis that radiation induces a DR depletion in osteocytes and an increase in empty lacunae. These reliable and reproducible metrics can now be utilized to determine the efficacy of therapies aimed at safeguarding the cells essential for optimal bone regeneration and potentially enhance the use of DO in HNC patients.

INTRODUCTION

An important clinical challenge in the use of ionizing radiation (XRT) in the treatment of patients with head and neck cancer (HNC) is to minimize injury to normal tissue within the treatment field. The changes induced in the surrounding tissues in the XRT field are a function of the XRT method, the amount of XRT therapy, the fractionation regimen, and the tissue type. Biologic effects therefore differ with different forms of XRT. In order to standardize the amount of XRT exposure to biologic tissues, a method of calculation has been devised that takes into consideration all of the variables previously outlined in order to arrive at a reliable and consistent biologic equivalent dose (BED). This BED is arrived at by taking the absorbed dose in Grays $_{\alpha/\beta}$ ($Gy_{\alpha/\beta}$) and multiplying by a XRT operational value or weighing factor which is dependent on the tissue type as described below by the linear quadratic (LQ) model[1]:

BED = $E/\alpha = n * d * (1 + d/(\alpha/\beta))$, where n=number of fractions, d=dose/fraction, nd=total dose, α represents the $\log_e$ of the cells killed per gray in the linear portion of the LQ curve, and β represents the $\log_e$ of the cells killed per gray squared or the quadratic component of cell killing as the curve bends. The ratio α/β has the dimensions of the dose and is the dose at which the linear and quadratic components of cell killing are equal.[2] The ratio α/β is a radiobiological characteristic that defines the sensitivity of a tissue to radiation dosage. Tissues (such as skin or mucosa) that are more susceptible to XRT injury or so-called early-responding normal tissue have an alpha/beta ratio of 10 Gy.[2] Conversely, late responding tissues such as bone have a lower ratio (<5 Gy). [2] Conventional therapy for HNC involves the use of high energy XRT with absorbed doses up to 70 Gy that are delivered via a fraction size of 1.8–2Gy.[3] Previous work in our lab has demonstrated significant impairment of new bone formation in the murine mandible after XRT most likely precluding the use of distraction osteogenesis as a viable reconstructive option for HNC patients.[4,5,6,7] An ideal XRT regimen would have its greatest effect on the primary target without altering the physiologic properties of adjacent tissues that are essential for adequate recovery and healing. Unfortunately, in HNC treatment, the mandible often falls victim to unintended and unwarranted XRT exposure, hindering its ability to generate new bone and heal. Although, there are well-documented reports on the damaging effects of ionizing XRT on bone regeneration, the literature is surprisingly deficient in outlining the effects of XRT on the histomorphometric properties of bone.

In an effort to address the paucity of the literature in regards to the effect of XRT on a clinically translational model that mimics the treatment regimen for HNC, we aimed to objectively measure the human equivalent dose response effects on the integrity of cellular and tissue composition in the murine mandible via the utilization of quantitative histomorphometry (QHM). Our In vivo model quantitatively analyzes the histopathologic effects of XRT on craniofacial membranous bone using a fractionated dosing schedule, in order to determine dose dependency. Specifically, we investigated the XRT induced changes at a BED that approximates the same dosage a human mandible is exposed to during

treatment for HNC. In an effort to establish a dose response, we also looked at a BED of both 75% and 150% of that seen clinically for HNC.

We hypothesize that the pathologic effects of XRT on regenerate formation are mediated through a mechanism of direct cellular depletion of the cells responsible for osteogenesis; furthermore we posit that the depletion of those cells will follow a dose response relationship.

MATERIALS & METHODS

20 Sprague-Dawley rats (~400 g) were obtained via the University of Michigan's Unit for Laboratory Animal Medicine (ULAM) department in compliance with the University of Michigan's Committee for the Utilization and Care of Animals (UCUCA). They were randomly assigned in three experimental radiation dosage groups: low dose (5.91 Gy; n=7), middle dose (7 Gy; n=7) and high dose (8.89 Gy; n=6) delivered in 5 daily fractions. These dosages were used so as to approximate 75%, 100%, and 150% respectively of the BED the mandible sees in the clinical regimen in HNC patients (Figure 1).

Animals

The animals were weighed, paired in cages and kept in a pathogen-free environment on a 12-hour light/dark schedule. Rats received standard soft chow and water ad Librium during a 7-day acclimation period prior to handling.

Radiation therapy

Prior to XRT, rats were anesthetized with a mixture of Oxygen-Isoflurane and placed right side down with a custom-designed lead shield over the body allowing exposure of the left posterior hemimandible. Fractionated external beam XRT at the experimental dosages mentioned above was performed on the rat left hemimandible over five days using a Philips RT250 orthovoltage unit (250 kV, 15 mA) (Kimtron Medical, Woodbury, Connecticut)[5]. An ionization chamber connected to an electrometer system was utilized for dosimetry (Figure 2).

As previously described in our irradiated murine mandibular model of distraction osteogenesis, 56 day-observation period followed, where the rats were fed soft chow and water ad Librium. [4,5,6,7] Rats exhibiting signs of radiation-related stress were injected subcutaneously with 10 cc Lactated Ringer containing buprenorphine (0.03m/kg).

Tissue processing and Radiographic examination

One death occurred in the high radiation dosage group. No other animals exhibited major adverse effects of radiation. The animals were sacrificed on the 56th day post-XRT and the left hemimandibles were harvested for histological evaluation. All specimens underwent ethanol fixation (70%) at 4°C then were rinsed in phosphate buffered saline. Specimens were decalcified with Cal-Ex®II (Fisher Scientific, Fair Lawn, NJ) (a mixture of 10.6% formic acid, 7.4% formaldehyde and <1% methyl alcohol) and stored at 4°C. The decalcification solution was changed every 2–3 days and the specimens were followed radiographically via self-contained Faxitron X-Ray (MX20, Faxitron X-Ray, Lincolnshire, IL) until full decalcification was achieved. The specimens were vacuum processed (dehydration and paraffin infiltration) under a 48 h program in the Hypercenter tissue processor (Shandon, Hypercenter XP, Pittsburg, PA), then filtrated once more for 2 hours in a vacuum bath (Leica Embedding Center, Model EG1160, Germany), followed by embedding in Paraplast Plus (i.e., paraffin containing Dimethysulfoxide, McCormic Scientific, Richmond, IL). Peel-a-way embedding molds, 22×40mm were used and stored

overnight at 4°C. Blocks were sectioned coronally from anterior to posterior into 7μm thick sections taken on a Leica Reichert-Jung microtome (Model 2030; Biocut, Bensheim, Germany) and mounted on glass slides (Fisherbrand Superfrost® Plus, Fisher Scientific, Pittsburg, PA). Sections were surface-stained with Gomori's "One step" Trichrome.

Histomorphometric evaluation

Point counting of osteocytes and empty lacunae was performed with a light microscope interfaced with a digital camera connected to a computer. Our region of interest (ROI), which spanned a distance of 5.1mm posterior to the 3rd molar was superimposed on the digital image using the imaging analysis software program Bioquant®NOVA Osteo version 7(R&M Biometrics, Nashville, TN). Nine high power field (HPF) images were randomly selected per ROI using 16× magnification. The HPF images measured 295×366 and were stored as TIFF files. Point counting of osteocytes and empty lacunae was performed by three independent reviewers.

Statistical analysis

Values were analyzed with a One-way ANOVA independent-samples Kruskal-Wallis test using SPSS for Windows version 16.0 (Chicago, IL). Results were statistically significant at a p value less than 0.05.

RESULTS

Clinical findings

During the recovery period, the low dose (LD) group animals tolerated XRT better than the other two groups. The LD group maximal weight loss of 32 g or 8% occurred between post-XRT days four and eleven with subsequent weight gain above the pre-treatment weight by day 56. XRT-induced alopecia was also less significant in this group (Figure 3A). The middle dose (MD) group animals lost about 63 g or 15.8% in a similar time frame. Those animals demonstrated more signs of mucositis and alopecia compared to the LD group (Figure 3B). In the high dose (HD) group, one animal did not survive; it represented the only animal loss in this experiment. The HD group animals lost up to 90 g or 22.5% of their pre-treatment weight. They also exhibited significant mucositis and alopecia (Figure 3C). Despite the initial dose response related morbidities all the animals eventually tolerated their diets and gained weight above their pre-treatment level. Overall, the mucositis was limited to the field of XRT (Figure 3) and resolved completely in the LD group but only partially in the remaining two groups. The animals progressively had partial hair regrowth at the irradiated site. IV hydration and pain management in all animal groups worked well to reverse severe signs of XRT-induced stress. At the time of harvest, gross inspection of the left hemimandibles demonstrated bony atrophy in proportion to XRT dosages; consistent with a dose response effect. Similar observations were made radiographically during the decalcification period. Those findings were reported to provide an overall clinical perspective to XRT damage, similar to those observed in humans.

Qualitative histological findings

Gomori Trichrome stain allowed digital color analysis, which demonstrated gross architectural variations among all the groups (Figure 4). The LD group displayed an abundant quantity of osteocytes within the surrounding waves of blue woven bone as compared to the osteocytes found in both the MD and the HD groups (Figure 4A). In addition, the osteocytes in the LD group demonstrated a less overall contracted appearance when compared to the two higher dose groups. Specimens from the MD group had a marked visible decrease in osteocytes as well as blood vessels and other hematopoietic elements in

comparison to the LD group. The bone in the MD group showed greater degrees of overall destruction, porosity, and bony injury in comparison to its LD counterpart (Figure 4B). The most severe loss of cellularity and vascularity was apparent in the HD group, which demonstrated profound changes across all specimens (Figure 4C). Overall, qualitative histological examination of XRT-induced changes to the mandible followed a dose response relationship with increasing levels of hypovascularity and hypocellularity clearly visible at increasing XRT dosages. We reported the aforementioned findings to provide additional information to the milieu in which the cellular damage is taking place.

Quantitative histomorphometric findings

The 16× magnification allowed clear distinction of the mature osteocytes within their respective lacunae. The mean number of osteocytes/HPF in the LD group was 57.57 ± 5.67. In the MD group, the mean number was reduced to 37.97 ± 5.98. Further reduction in osteocytes was observed in the HD group with a mean number of 29.94 ± 2.18. Overall, the decrement in the mean number of osteocytes was appreciated with increasing XRT dosages. The medians of osteocytes across all groups demonstrated statistical significance with the independent-samples Kruskal-Wallis test ($p=0.001$; Figure 5).

Empty lacunae were seen as a classic and distinct compartment or cavity within the bone matrix devoid of a residential osteocyte. The mean number of empty lacunae/HPF for the LD group was 0.71± 0.95. An expected increase in the mean number was observed in the MD group with a value of 3.57 ± 2.76. Further increase was seen in the HD group with a value of 5.16 ± 4.2. The independent-samples Kruskal-Wallis test also revealed a statistically significant difference between all groups when comparing the medians of empty lacunae in bony specimens ($p=0.037$; Figure 6).

DISCUSSION

XRT-induced histological changes in bone have been reported in several experimental studies, which involved rats, rabbits, monkeys, and dogs. [8,9,10,11] Unfortunately, most of the studies examining the tissue effects of XRT on normal bone have been qualitative in nature and have eschewed quantitative analyses. Quantitative measures of the histopathologic effects of XRT on the bones of the craniofacial skeleton have yet to be delineated in an in vivo model. Maeda et al.[8] found diminution in bone porosity, osteocytes and periosteal new bone in an in vivo model using male Sprague Dawley rat femora at 6–10 weeks following a single XRT dose of 3500 rads (35 Gy). Sugimoto et al.[12] reported synchronous changes of damage in intracortical porosity and endosteal new bone formation in Japanese white rabbit tibiae at 12 weeks after a single electron beam XRT dose of 50 Gy. The few studies that have evaluated the histopathologic effects of XRT on bone have centered predominantly on the effects on endochondral long bones and on single dosing regimens that do not translate well to the clinical treatment of HNC, which uses a fractionated dosing schedule that involves exposure of mainly membranous cortical bones.

Other studies exploring the fate of irradiated vascularized grafts, bone implants and alloplastic implants have made indirect correlations between XRT and subsequent histological changes. Evans et al.[9] subjected canine mandibular bone grafts to a total XRT dose of 40 Gy delivered in 12 fractions, three times weekly for 4 weeks. Their study showed a decrease in osteocytes within the cortex of both vascularized and non vascularized irradiated grafts. Lehner et al.[13] investigated the healing of vascularized long bone osseous transplants to irradiated recipient sites (total dose of 50 Gy delivered in 5 fractions of 10 Gy) using a pedicled tibia flap in the rat. They suggested that bone healing and bony union in an irradiated field were dependent on a minimum number of surviving osteogenic cells in the

recipient bone. Because these studies focused on bone grafts they shed little light on the histopathologic effects of XRT on normal bone.

In vitro studies have indirectly evaluated the effects of XRT on bone cellularity. Most of those studies involved the delivery of various XRT schemes to osteoblast-like cells. Matsumura et al.[14] conducted an investigation using a clonal osteoblastic cell line MC3T3-E1 and subjected them to XRT dosages of 1–10 Gy. They found that irradiation led to a greater number of more highly differentiated osteoblasts and also inhibited overall cell proliferation; both of which led to impaired bone growth. Dudziak et al.[15] performed a similar experiment using varying dosages of ionizing XRT (0–8 Gy). They showed a diminution of growth factor production, and speculated that such findings could result in impaired osseous healing. They also found a XRT dose-dependent inhibition of cell proliferation and increased alkaline phosphatase consistent with Matsumura et al.[14] Such dose dependency, however, has never been extended nor verified in vivo.

In an attempt to address the shortcomings in previous models we endeavored to quantitatively evaluate the cellular and structural effects of XRT using QHM as an objective and reproducible analytical method. QHM remains the gold standard to objectively gauge the effects of XRT on tissue and cellular composition. Furthermore, we explored the question as to whether those effects on bone followed a dose response pattern. In order to maximize the translational nature of this study we were able to examine the effects of XRT dosages in the murine mandible that approximated the bioequivalent doses a human would receive in HNC. In addition, we added a fractionation schedule to our model in order to better mimic the conventional scenario that is found in the clinical arena.

Utilizing QHM, the present study demonstrates XRT induced dose-dependent alterations in bone cellularity that is reproducible in a murine mandibular bone. Our data demonstrates a decrease in osteocytes with increasing XRT dosages. Osteocytes are the bone-forming cells that originate from osteoblast terminal differentiation. They inhabit inner lacunae, and they are the most abundant cells in bone. Their striking morphological characteristics are an excellent predictor of their role in bone remodeling in response to mechanical stress, fatigue or radiation. Specifically, in radiotherapy, osteocyte death frequently correlates clinically with the diagnosis of osteoradionecrosis-ORN[15].

The mandible is a highly cortical membranous bone with very little blood supply. Therefore, XRT-induced alteration in its architectural backbone, will intimately affect both remodeling capacity and biomechanical properties. Studies of XRT induced damage on cortical bone have shown that XRT initially affected vascular patency, followed by bone resorption, diminution of viable osteocytes, and then bone remodeling. [1,16] The osteocytes are thought to be a radioresistant type cell,[2] whose death after radiotherapy can be attributed chiefly to vascular damage. The deprivation of those cellular components, the loss of vascularity and osteoid formation all contribute to an impaired bone remodeling.

In addition to our findings described above, our data also delineates a quantifiable XRT dose-dependent increase in empty osteocyte lacunae. Empty lacuna is the compartment occupied by an osteocyte in the bone matrix, also called osteoplast. Therefore, empty osteocytic lacunae are a reliable account of osteocyte death.[17] Takahashi et al.[18] have observed a tendency of clustering of the empty lacunae around an obliterated Haversian canal in endochondral femoral condyles suggesting again that XRT-induced osteocyte death involved vascular damage.

Rohrer et al.[11] have looked at the effect of cobalt-60 irradiation on rhesus monkey mandibles (45 Gy fractionated into 10 sessions over 12 day-period). The animals were euthanized within one to six months after radiotherapy, and the percentage of empty

osteocytic lacunae was recorded at each histological section. They found that osteocytes were lacking in cortical bone lacunae and in Haversian bone. The death of osteocytes was directly attributed to radiation effect as it occurred in the direct path of the XRT beam. Unfortunately, this study involved very small numbers without any valid statistical analysis; a significant limitation most likely related to their use of a large animal model.

Pelisser et al.[19], a Brazilian group, have also performed a microscopic analysis of fractionated cobalt-60 radiotherapy (60 Gy delivered in 30 sessions at 2Gy/day-doses) on murine mandibles. They found an increase in the mean percent number of empty lacunae in comparison to non-irradiated control rats. Both the Rohrer and Pelisser studies did not use QHM to directly measure osteocytes, they did not address the issue of dose response, and their models were not optimal because they used Cobalt-60 as a XRT delivery model. Modern evidence on the use of Cobalt-60 remains anecdotal at best in few reported clinical cases. Cobalt-60 is considered an old treatment modality that yet has to be modernized, it is less uniform, more highly scattered, and produces a lower amount energy.[20,21]

Our lab previously demonstrated that XRT significantly alters new bone formation in the murine mandible impeding the use of distraction osteogenesis as a viable reconstructive treatment option after radiation therapy.[4,5,6,7] In order to better understand the diminished bone quality within the irradiated mandible that contributes to impaired osteogenesis and repair, we investigated specific metrics of bone degradation that could be subsequently mitigated to allow functional restoration and successful regeneration of the craniofacial skeleton. By means of QHM we objectively measured the XRT induced cellular and tissue changes in the membranous bone of the murine mandible utilizing a XRT method, a fractionation regimen, and a bioequivalent dose that approximates the same conditions a human mandible is exposed to during treatment for HNC. The findings in this report support our hypothesis that the deleterious effects of XRT are mediated through a dose response depletion of essential osteogenic cells. The long term goal of this work is to provide fundamental information that can be translated from the bench to the bedside to lead to improved treatment modalities for patients suffering from the disastrous sequelae of XRT therapy. More specifically, therapies will be introduced aimed at preserving the osteogenic cells, and similar QHM will be performed to determine the efficacy of those therapeutic interventions to increase or decrease cellularity quantitatively.

CONCLUSION

This study supports our hypothesis that XRT impedes new bone formation by inducing cellular depletion and eliminating the cells responsible for osteogenesis. Our findings also establish a dose response effect in regards to XRT, specifically measuring the degree of severe attenuation of cellularity within the murine mandible. Future studies can now be performed, utilizing these metrics, to determine the efficacy of therapies aimed at safeguarding the cells essential for optimal bone regeneration.

Acknowledgments

We thank Sagar Deshpande for his help during surgery, and animal care. We also thank Charles Roehm and John Baker for their technical assistance in the preparation of the external fixator/distractor, and preparation of the tissues for histologic analysis respectively. We particularly thank Mary Davis, Dr. Avraham Eisbruch and Dr. Ted Lawrence for their expertise in radiation oncology.

Funding supported by the following grant:

“Optimization of Bone Regeneration in the Irradiated Mandible”, NIH-R01#CA 125187-01, PI: Steven R. Buchman.

References

1. Jegoux F, Malard O, Goyenvalle E, Aguado E, Daculsi G. Radiation effects on bone healing and reconstruction: interpretation of the literature. Oral Surg Oral Med Oral Pathol Oral Radiol Endod. 2010; 109(2):173–184. [PubMed: 20123406]
2. Hall, EJ. Radiobiology for the Radiologist. Ed. 6. Philadelphia: J.B. Lippincott; 2006.
3. Fränzel W, Gerlach R. The irradiation action on human dental tissue by X-rays and electrons – a nanoindenter study☆. Z Med Phys. 2009; 19(1):5–10. [PubMed: 19459580]
4. Fregene A, Jing XL, Monson LA, Buchman SR. Alteration in volumetric bone mineralization density gradation patterns in mandibular distraction osteogenesis following radiation therapy. Plast Reconstr Surg. 2009 Oct; 124(4):1237–1244. [PubMed: 19935308]
5. Fregene A, Jing XL, Monson LA, Buchman SR. quantitative histomorphometric assessment of regenerate cellularity and bone quality in mandibular distraction osteogenesis following Radiation Therapy. J Craniofacial Surg. 2010 Sept; 21(5):1438–1442.
6. Schwarz DA, Arman KG, Kakwan MS, et al. Regenerate healing outcomes in unilateral mandibular distraction osteogenesis (MDO) utilizing quantitative histomorphometry (QHM). Plast Reconstr Surg. 2010:795–805. [PubMed: 20463629]
7. Schwarz DA, Jamali AM, Kakwan MS, et al. Biomechanical assessment of regenerate integrity in irradiated mandibular distraction osteogenesis. Plast Reconstr Surg. 2009; 123 2 Suppl:114S–22S. [PubMed: 19182670]
8. Maeda M, Bryant MH, Yamagata M, Li G, Earle JD, Chao EY. Effects of irradiation on cortical bone and their time-related changes. A biomechanical and histomorphological study. J Bone Joint Surg Am. 1988; 70(3):392–399. [PubMed: 3346264]
9. Evans HB, Brown S, Hurst LN. The effects of early postoperative radiation on vascularized bone grafts. Ann. Plast. Surg. 1991; 26:505–510. [PubMed: 1883154]
10. Gowgiel JM. Experimental radio-osteonecrosis of the jaws. J Dent Research. 1960 Jan–Feb. 39:176–197. [PubMed: 13828645]
11. Rohrer MD, Kim Y, Fayos JV. The effect of cobalt-60 irradiation on monkey mandibles. Oral Surg Oral Med Oral Pathol. 1979 Nov; 48(5):424–440. [PubMed: 114905]
12. Sugimoto M, Takahashi S, Toguchida J, Kotoura Y, Shibamoto Y, Yamamuro T. Changes in bone after high-dose irradiation Biomechanics and histomorphology. J Bone Joint Surg Br. 1991 May. 73-B:492–497. [PubMed: 1670456]
13. Lehner B, Bauer J, Rödel F, Grabenbauer G, Neukam FW, Schultze-Mosgau S. Radiation induced impairment of osseous healing with vascularized bone transfer: experimental model using a pedicled tibia flap in rat. Int J Oral Maxillofac Surg. 2004 Jul; 33(5):486–492. [PubMed: 15183413]
14. Matsumura S, Jikko A, Hiranuma H, Deguchi A, Fuchihata H. Effect of X-ray irradiation on proliferation and differentiation of osteoblast. Calcif Tissue Int. 1996 Oct; 59(4):307–308. [PubMed: 8781058]
15. Dudziak ME, Saadeh PB, Mehara BJ, et al. The effects of ionizing radiation on osteoblast-like cells in vitro. Plast Reconstr Surg. 2000; 106:1049–1061. [PubMed: 11039376]
16. King MA, Casarett GW, Weber DA. A study of irradiated bone: I. Histopathologic and physiologic changes. J Nucl Med. 1979; 20:1142–1149. [PubMed: 536774]
17. Mullender MG, van der Meer DD, Huiskes R, Lips P. Osteocyte density changes in aging and osteoporosis. Bone. 1996; 18:109–113. [PubMed: 8833204]
18. Takahashi S, Sugimoto M, Kotoura Y, Sasai K, Oka M, Yamamuro T. Long-term changes in the haversian systems following high-dose irradiation: An ultrastructural and quantitative histomorphological study. J Bone Joint Surg Am. 1994; 76:722–738. [PubMed: 8175821]
19. Pelisser, A.; Vier-Pelisser, FV.; Fontanella, VR.; Zancarno de Figueiredo, MA. Radiol Bras. Vol. 40. 2007. Microscopical analysis of fractionated cobalt-60 radiotherapy effects on mandibles of rats; p. 113-118.
20. Dyk JV, Battista JJ. Cobalt-60 : An old modality, a renewed challenge. Cur Oncol. 1996; 3:1–31.
21. Joshi CP, Dhanesar S, Darko J, Kerr A, Vidyasagar PB, Schreiner LJ. Practical and clinical considerations in Cobalt-60 tomotherapy. J Med Phys. 2009; 34:137–140. [PubMed: 20098560]

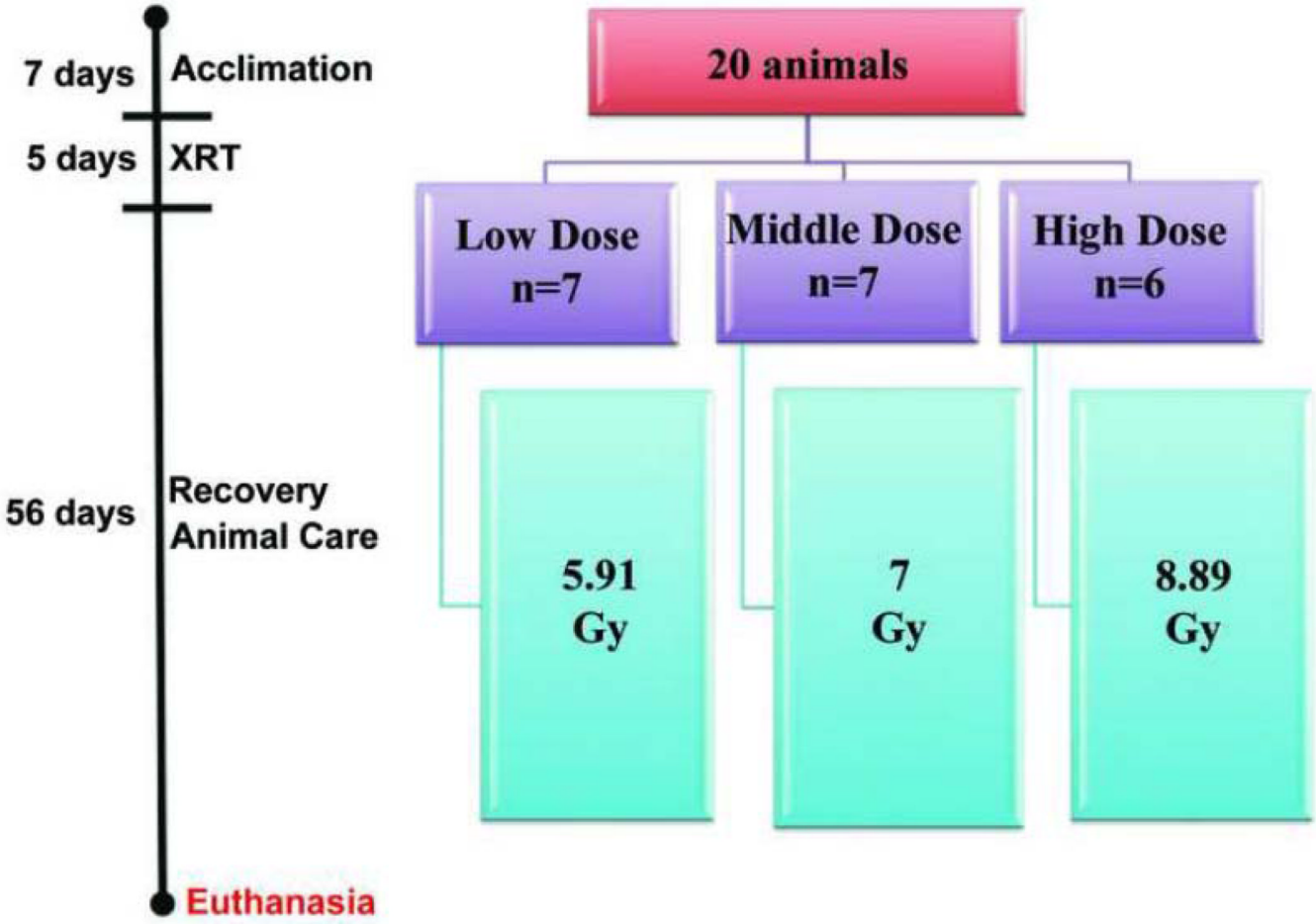

Figure 1.
Experimental Design and Timeline

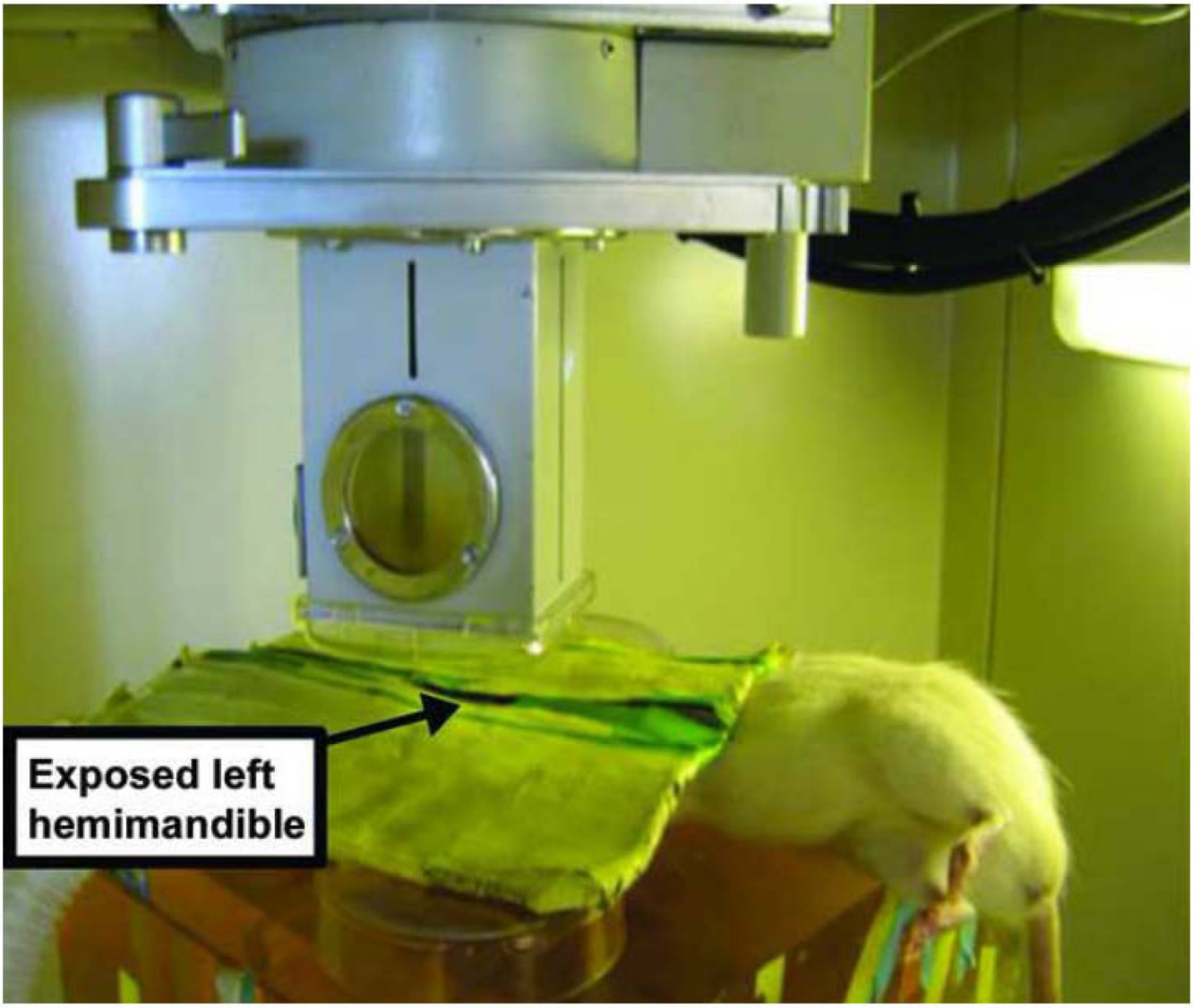

Figure 2.
Sprague Dawley male rat undergoing left hemimandible radiation. Custom-designed lead shield protecting the remainder of the rat.

Figure 3.
Rats demonstrating radiation-induced alopecia at low dose XRT (A), middle dose XRT (B) and high dose XRT (C).

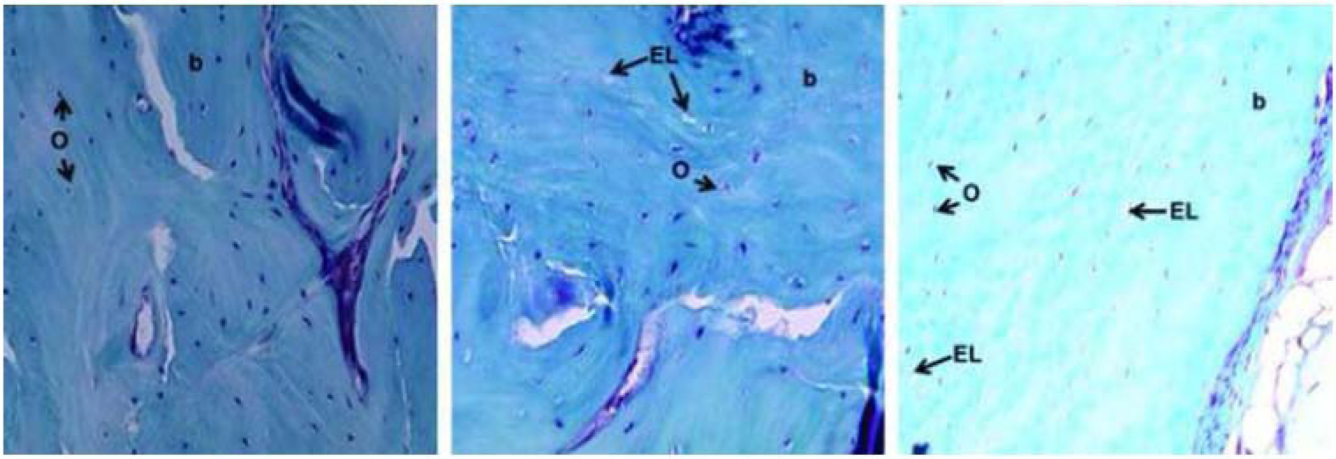

Figure 4.
Qualitative Histologic Findings. Digital photograph at 16× magnification showing bone, osteocytes within lacunae and empty lacunae with Gomori Trichrome stain at low dose XRT (A), middle dose XRT (B) and high dose XRT (C).

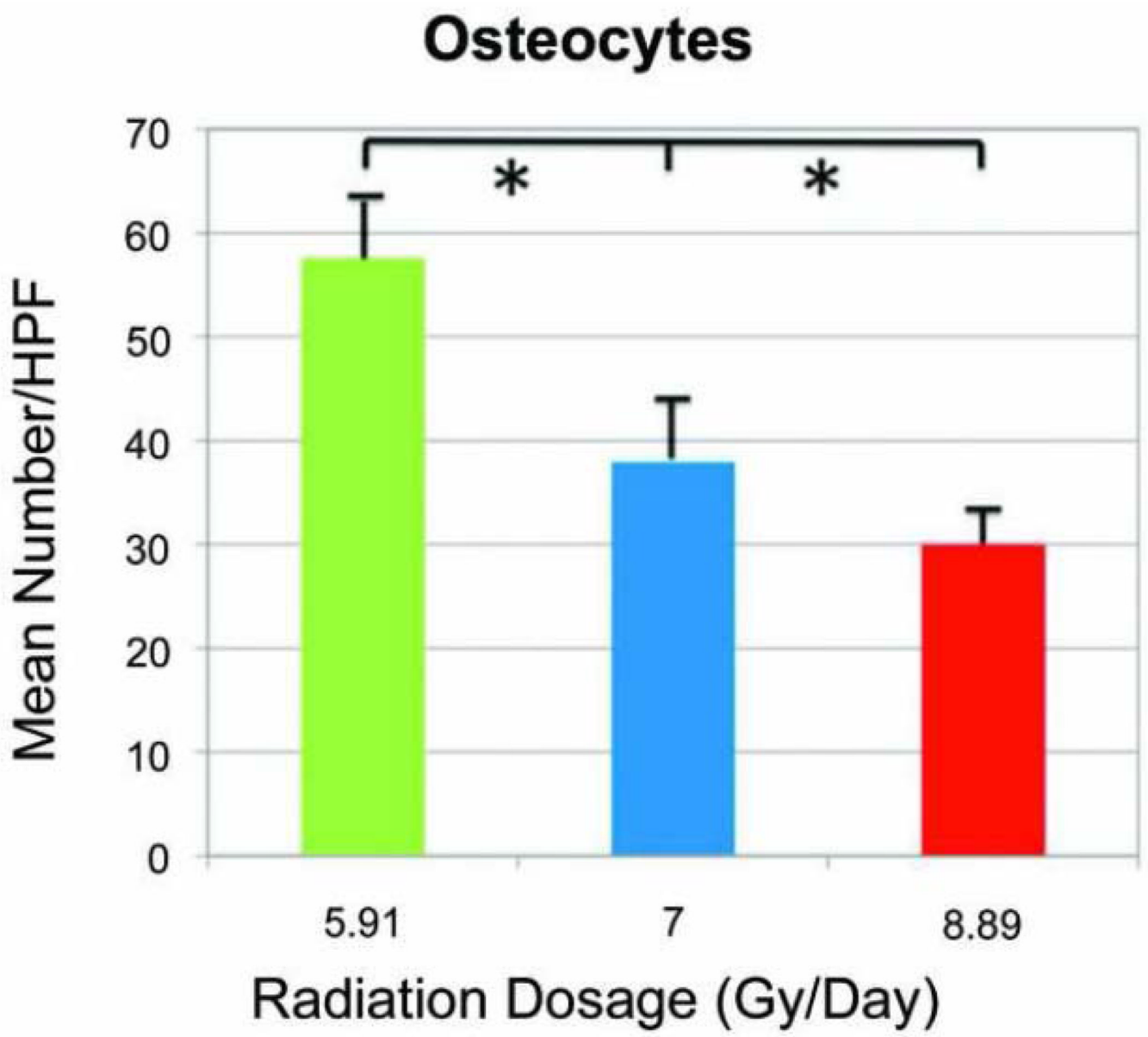

Figure 5.
Number of osteocytes per high power field (HPF) at increasing radiation dosage.

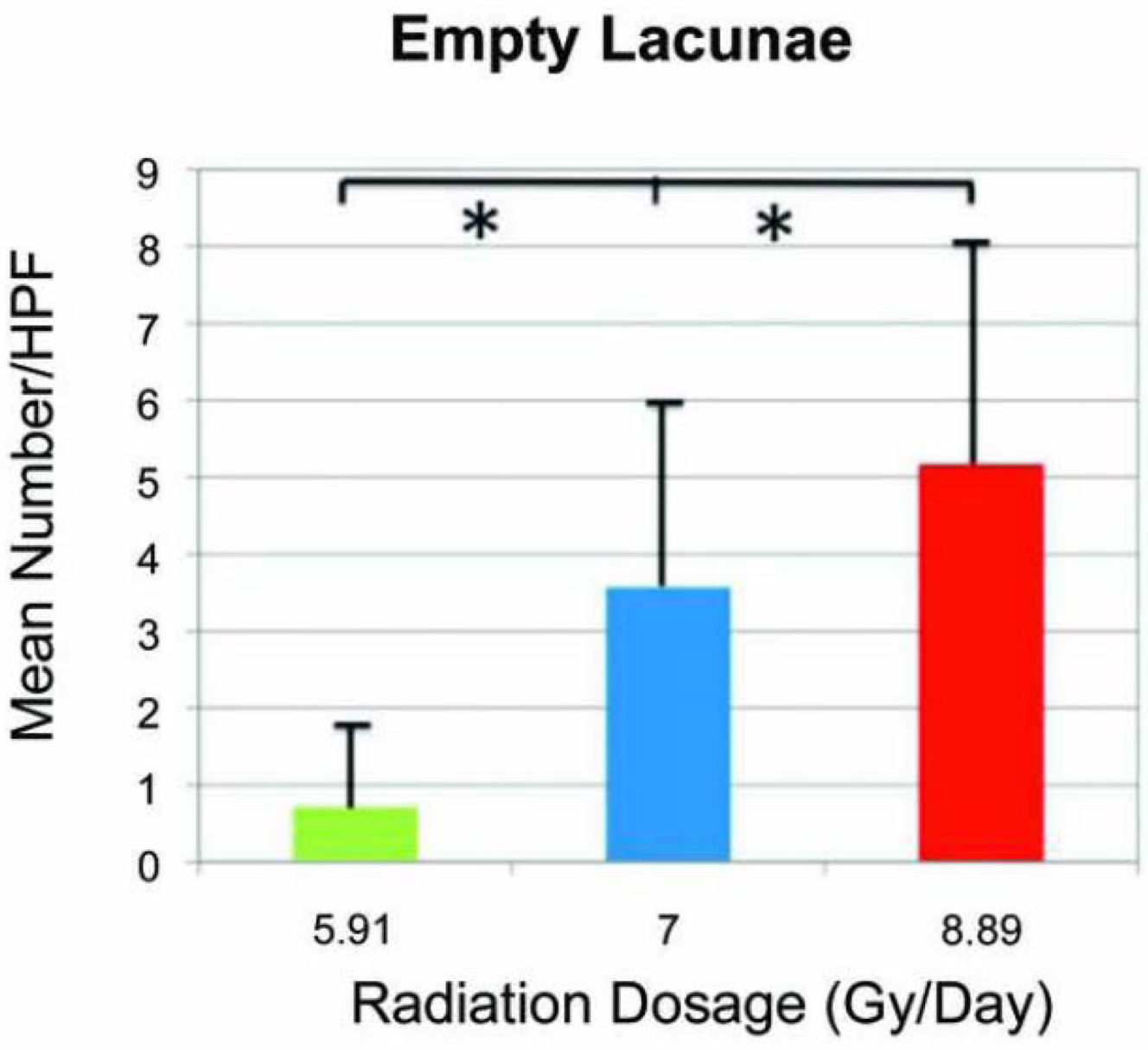

Figure 6.
Number of empty osteocytic lacunae per high power field (HPF) at increasing radiation dosage